Computers and Electronics in Agriculture 221 (2024) 109009

Contents lists available at ScienceDirect

Computers and Electronics in Agriculture

journal homepage: www.elsevier.com/locate/compag

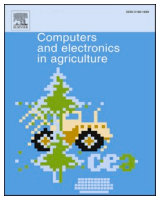

Downscaled numerical weather predictions can improve forecasts of sugarcane irrigation indices

Andrew Schepen [a,*], Justin Sexton [b], Bronson Philippa [d], Steve Attard [e], David E. Robertson [f], Yvette Everingham [c,d]

[a] Commonwealth Scientific and Industrial Research Organisation, Dutton Park, Australia
[b] Commonwealth Scientific and Industrial Research Organisation, Townsville, Australia
[c] Agriculture Technology and Adoption Centre, James Cook University, Townsville, Australia
[d] College of Science and Engineering, James Cook University, Townsville, Australia
[e] AgriTech Solutions, Ayr, Australia
[f] Commonwealth Scientific and Industrial Research Organisation, Clayton, Australia

ARTICLE INFO

Keywords:
Crop simulation
Decisions support
Forecast post-processing
Ensemble verification
APSIM
Weather forecasting

ABSTRACT

Efficient irrigation reduces energy and water costs, increases profit margins and delivers better environmental outcomes. Whilst many growers rely on weather forecasts to make decisions, few studies have sought to incorporate weather forecast uncertainty into the optimisation of irrigation management or to evaluate weather forecasts through the lens of irrigation indices. Therefore, in this study, we seek to generate and evaluate ensemble forecasts of irrigation indices produced by coupling numerical weather prediction (NWP) forecasts with a biophysical process model (APSIM). We investigate a case study application for sugarcane in northeastern Australia. As a first step, three and a half years of forecasts from the Australian Bureau of Meteorology's ACCESS-G3 model are statistically post-processed to generate 7-day forecasts that are downscaled and calibrated to local climate zones. In addition, the forecast post-processor converts the deterministic forecasts into an ensemble, thus quantifying forecast uncertainty. The generated forecasts are then used as forcing for the APSIM crop model to produce ensemble forecasts of soil water deficit (SWD), crop water use (CWU) and crop stress (Stress) for a simulated sugarcane crop. Through cross-validation, the post-processed weather forecasts demonstrate improved forecast accuracy compared to naive climatology and raw NWP forecasts for daily rainfall, maximum and minimum temperature and solar radiation; with the added benefit of providing a reliable uncertainty estimate. Improvement to an even greater degree is observed for the derived irrigation indices, particularly CWU and Stress, for which the forecasts are also reliable. The developed irrigation indices based on NWP can be used directly for decision making or, alternatively, may be used further in machine learning for optimisation of irrigation schedules in conjunction with other remotely sensed variables.

1. Introduction

Irrigation efficiency gains are necessary to combat pressures on water availability, farm business and environmental outcomes associated with population growth, climate change, water quality (Waterhouse et al., 2017) and the rising costs of energy and water (e.g. Belaud et al., 2020; Fader et al., 2016). Pumping less water can also save energy and contribute a vital step to help farmers reach net zero sooner (Rosa & Gabrielli, 2023). At the farm scale, more efficient irrigation can be achieved through improvements to irrigation technology and better decisions around irrigation scheduling, especially with consideration to the prevailing and future soil, crop, and atmospheric conditions (Gu et al., 2020).

In recent years, the combination of in-field sensors and machine learning (ML) techniques led to the development of fully automated irrigation systems in smart irrigation projects (e.g. Domínguez-Niño et al., 2020; Gu et al., 2021; Wang et al., 2020). Typically, such systems rely on real-time, in-situ measurements of soil moisture and weather conditions but ignore oncoming changes in the weather that may bring increased rainfall or evapotranspiration. A counter example is Goap et al. (2018), who piloted an irrigation system that used ML to predict soil moisture using weather forecasts and to automate irrigation

* Corresponding author.
E-mail address: andrew.schepen@csiro.au (A. Schepen).

https://doi.org/10.1016/j.compag.2024.109009
Received 21 January 2024; Received in revised form 10 March 2024; Accepted 1 May 2024
Available online 5 May 2024

decisions such as delaying irrigation or applying minimum water until rain arrives. However, the system did not consider uncertainty in the weather forecast.

There is evidence that the use of weather forecasts can lead to improved irrigation outcomes (Wang & Cai, 2009). For example, Cao et al. (2019) considered a water-balance and evapotranspiration model in conjunction with 3-day rainfall forecasts to optimise irrigation scheduling for a rice-paddy application in China, finding that forecast-based decisions saved significant volumes of water and reduced drainage whilst preserving yields. Anupoju et al. (2021) and Gedam et al. (2023) investigated the skill of 5-day rainfall and ET_0 forecasts in India, who also found that the use of the forecasts led to significant water savings and improved yields. Guo et al. (2022) considered 9-day rainfall forecasts to simulate outcomes of irrigation decisions for a maize field in Australia. A unique aspect of this study was that rainfall uncertainty was included by using ensemble rainfall forecasts generated by post-processing deterministic numerical weather prediction (NWP) forecasts. The rainfall ensembles were propagated through a biophysical model (APSIM) to generate outcomes of soil water, runoff, and drainage. However, the study did not post-process weather forecasts for the other requisite APSIM inputs of temperature and solar radiation, and instead used actual observations. A true forecasting system will need to include forecasts of all the requisite weather variables and consider their covariance.

As a step towards a more complete system incorporating uncertainty, we investigate the post-processing of NWP forecasts of rainfall, temperature, and solar radiation, plus the extension to forecasts of irrigation indices including soil water deficit (SWD), crop water use (CWU) and crop stress (Stress). The irrigation indices are produced by filtering weather data and forecasts through a biophysical process model (APSIM).

Direct assessments of forecasts of irrigation indices will help to develop a fundamental understanding of the relationship between NWP and the accuracy and reliability and of forecast irrigation indices. Another benefit, as noted by Guo et al. (2022), is that a farmer may occasionally want to stress a crop or take other unusual action for operational reasons, to which end irrigation indices are a more useful product than an optimised schedule. An optimised schedule would also need to consider each farm's individual constraints in terms of irrigation infrastructure, the time required to irrigate different paddocks, the number of blocks that can be irrigated simultaneously, and any chosen time-of-use energy tariffs (Wang et al., 2020). Additionally, some growers simply prefer a more "hands on" approach to decision making and appreciate a panel of information such as accumulated rainfall totals, soil moisture levels and other indicators such as those generated in this study. Nevertheless, irrigation indices can become inputs to machine learning models, and it will be useful to understand a priori the skill of forecasts to identify the most appropriate indices to include in fully automated climate-smart irrigation systems.

NWP models are developed on coarse grids and thus do not capture variability at the farm scale, whilst also being susceptible to systematic biases and model structural errors. For example, the Australian Bureau of Meteorology's ACCESS-G3 model, which we will use, operates at a scale of roughly 12 km and parameterises rainfall. The spatial scale problem can be addressed by downscaling raw forecasts to match observations at a finer resolution for a given spatial region. Forecast calibration methods can be applied to address biases and other systematic errors. For example, Bayesian joint probability modelling (BJP) has been applied to post-process daily rainfall forecasts from earlier versions of ACCESS-G to match hydrological catchment rainfall (Robertson et al., 2013; Shrestha et al., 2015). As a model output statistics approach, BJP also samples forecast uncertainty and can be used to generate multiple rainfall futures in the form of ensembles. Rainfall forecasts from ACCESS-G have been post-processed with other methods such as quantile mapping in wavelet-transformed space (Jiang & Johnson, 2023), spatial-mode calibration (Zhao et al., 2022) and seasonally-varying calibration.

In our work, the development of forecasts for APSIM requires multiple weather variables and therefore multivariate forecast calibration methods are needed. Multivariate post-processing ensures each member in the forecast has realistic temporal, spatial and/or intervariable patterns (Lakatos et al., 2023; Schepen et al., 2020c; Whan et al., 2021). Recent research has extended the Bayesian joint probability modelling approach for calibrating and downscaling multivariate seasonal forecasts; employing the Schaake Shuffle to connect ensemble members across space, lead times and climate variables; with applications to APSIM simulations (Potgieter et al., 2022; Schepen et al., 2020a–c). We adopt a similar approach to post-process NWP variables in this study. As such, the main objectives of this study are to: (1) establish a framework for generating locally-relevant ensembles of rainfall, temperature and solar radiation, that can be used to predict irrigation indices and describe the uncertainty of these predictions; and (2) verify the performance of the weather forecasts and the corresponding irrigation indices, including soil water deficit (SWD), crop water use (CWU) and crop stress (Stress). We select a case study of an APSIM sugarcane model in northeastern Australia, which is representative of irrigated farms in the Burdekin region, a major cane growing region in Australia, situated adjacent to the Great Barrier Reef for which a climate-smart automated irrigation system is being developed (https://opticane.net). In sections 2 we present the data and methods. Section 3 presents the results. Sections 4 and 5 wrap up the paper with discussion and conclusions, respectively.

2. Study area and data

2.1. Study area

The study area is the Burdekin sugarcane growing region in northeastern Australia, which surrounds the Burdekin River (Fig. 1, panel 1). For the purposes of this study, the extent of sugarcane cropping was identified from land use data made available from the Queensland land use mapping series (Department of Environment and Science, 2023)). The Burdekin catchment experiences highly seasonal rainfall, with the "wet" season occurring November-April and the "dry" season in the remaining months. Water for the irrigation of over 50,000 ha of farmland is managed from the upstream Burdekin Falls Dam. Whilst water availability is generally only a concern during significant drought, estimates are that demand may exceed dam capacity by 2031 (Sun Water, 2022). Furthermore, the river discharges directly into the world heritage Great Barrier Reef. Therefore, the region requires efficient irrigation practices to reduce excess water leaving the paddock (Waterhouse et al., 2017).

2.2. Observed data

Observed data for daily rainfall, minimum daily temperature, maximum daily temperature, and solar radiation are extracted from the Australia-wide SILO 5 km gridded dataset https://silo.longpaddock.qld.gov.au/. Silo data correspond to 9 am – 9 am intervals. These data are used in two ways. Firstly, to divide the Burdekin into distinct climate zones through a cluster analysis and secondly, as a training and verification dataset for the forecast post-processing. For the purposes of climate zone identification, data from 1970 to 2010 were used. For the purposes of forecast post-processing, data from 2019 to 2023 are used. The reasons for the different periods are that the climate zone analysis requires a long data record whereas the forecast post-processing data needs to align with the available NWP dataset, which is relatively recent. Once the climate zones have been identified, the SILO data for the forecasting experiments is area-averaged within each climate zone at a daily time step.

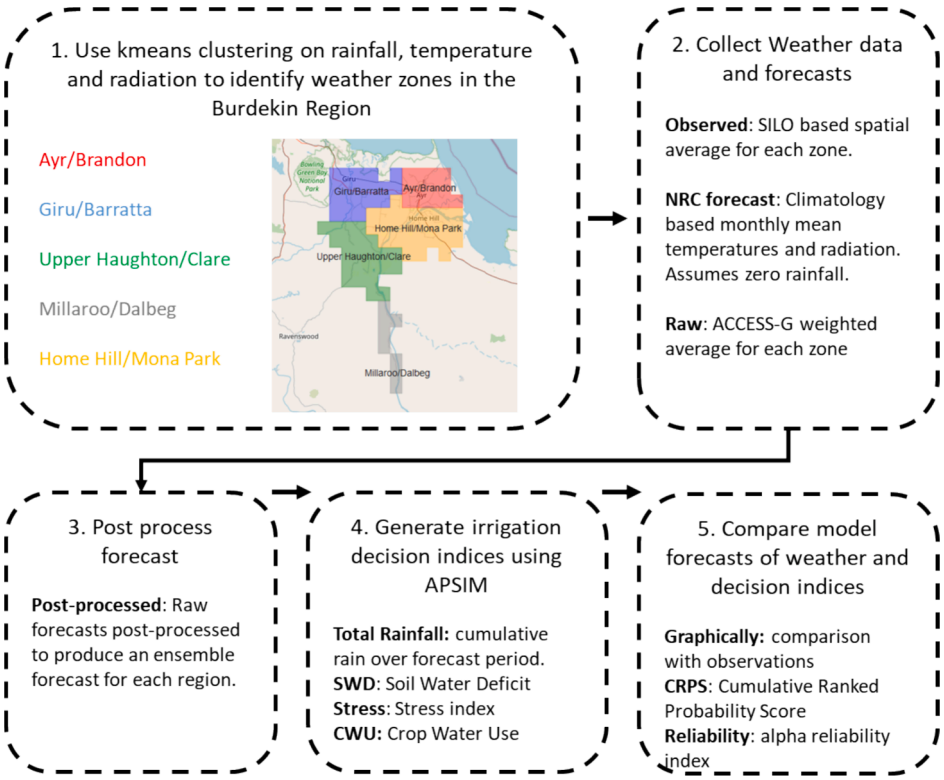

Fig. 1. . Outline of study methodology for climate zone identification, forecast post-processing, irrigation index generation and forecast verification.

2.3. Forecast data

Numerical weather prediction forecasts of rainfall, temperature and solar radiation are sourced from the Bureau of Meteorology ACCESS-G3 dataset hosted on the National Computational Infrastructure (https://dapds00.nci.org.au/thredds/catalog/wr45/ops_aps3/access-g/1/catalog.html). These forecasts are highly suitable for statistical post-processing because they are deterministic, numeric time series and are free from human manipulation. ACCESS-G3 is initiated four times per day at 00Z, 06Z, 12Z and 18Z. For operational reasons, the 12Z dataset is selected, which corresponds to approximately 10 pm local time, meaning that for real-time operation, the forecast has time to complete and be post-processed for release the following morning. The hourly NWP data are processed to calculate minimum and maximum temperatures and 24-hour rainfall and solar radiation up to 7 days ahead (i.e. 1–7 days lead time), aligning with the 9 am to 9 am window of SILO data.The daily forecasts are subsequently area-averaged for each climate zone and paired with a SILO observation for the corresponding 24-hour period.

2.4. Climate zones

Local climate zones are identified within the study region using a k-means clustering approach on SILO rainfall, temperature and solar radiation using the method developed by Sexton et al. (2017). The number of clusters was investigated in consultation with industry partners and a five-cluster solution is used (Fig. 1, panel 1). From north-west to north-east, the five zones are identified as Giru/Barratta, Upper Haughton/Clare, Millaroo/Dalbeg, Home Hill/ Mona Park and Ayr/Brandon. The northern zones tend to be wetter with the north-western Giru/Barratta zone being the wettest region and the southern Millaroo/Dalbeg zone being the driest.

3. Methods

3.1. Overview of methodology

A schematic of the methodological workflow is illustrated in Fig. 1. Historical data for each climate zone are pre-processed as described in section 2.2. Additionally, a set of no rainfall climatology (NRC) “forecasts” for comparison purposes are calculated as zero rainfall and monthly climatological means for temperature and solar radiation. These forecasts reflect an uninformative baseline forecast similar to what may be used in irrigation decision support tools in the region (Sexton et al., 2022). The NWP weather forecasts are post-processed under a cross-validation framework with SILO data as the target, omitting 31 consecutive days surrounding the target forecast period The ensemble forecasts are then used as forcing for an established APSIM model with the irrigation indices calculated from the APSIM output variables. Probabilistic forecast verification techniques are then used to assess both the weather forecasts and the irrigation indices. Additional details are provided below.

3.2. Weather forecast post-processing

A Bayesian joint-probability model is used to model the joint distribution between raw ACCESS-G3 forecasts and SILO observations for each forecast day ahead (e.g. Robertson et al., 2013; Shrestha et al., 2015; Wang, Shao, et al., 2019). Specifically, we use the Gibbs-sampler implementation of BJP described by Wang,Shao,et al., (2019). For each weather variable, the joint distribution between the raw NWP forecast and the corresponding observation is assumed to follow a bivariate normal distribution after allowing for a normalising and variance-stabilising transformations of the predictor and predictand variables. For rainfall, the log-Sinh transformation is used (Wang et al., 2012). For temperature and solar radiation, the Yeo-Johnson transformation is used (Yeo & Johnson, 2000). Transformation of each variable is done independently as a first step using Bayesian *maximum a posteriori* estimation.

Then, the Gibbs sampler estimates the posterior distribution of the bivariate normal distribution parameters as a second step. In both steps, the prior distributions for the Bayesian inference are deliberately set to vague (wide or non-informative) distributions so that the parameters are determined mainly from the data.

The lower bound on rainfall presents a problem in that the distribution is not continuous (i.e. it has a probability mass at the lower bound). This problem is handled by setting a left censoring threshold. Censoring assumes that, theoretically, the actual value is at or below the censor threshold, and thus allows the use of the convenient continuous normal distribution instead of more complicated structures such as mixed-discrete distributions. We set the censoring threshold to zero.

BJP is applied to generate 200 ensemble members for each climate zone for lead times from 1 to 7 days. The Schaake shuffle (Clark et al., 2004) is then applied to inject realistic space–time and inter-variable correlations in the ensemble. As demonstrated by Schepen et al., (2020a) the Schaake Shuffle can generate suitable input series for APSIM by reordering the ensemble members according to the ranks of historically observed data, which will be correlated to some degree across space, time and variables.

A cross-validation approach was used to ensure that data surrounding the forecast issue date was not influential in the forecast training. In this study, data for the forecast initialisation day and 15 days either side were left out for the model fitting.

3.3. APSIM modelling

For each climate zone, a sugarcane crop is simulated using the Sugar module (Keating et al., 1999; Lisson et al., 2000) of APSIM V7.10 (Holzworth et al., 2018). The crop is first planted on 15 August 2019 with a simulation end date of 15 February 2023. This represents a late planted crop followed by three annual ratoons (the third ratoon crop is not grown to end of season). To supply nutrients, the cycle is fertilized with 500 kg/ha of urea fertilizer one month after sowing/ratooning. For all climate zones, a single soil type is used. The soil is characterized as a silty loam and has a plant available water content of 162 mm.

An automated irrigation cycle is implemented that applies 60 mm of irrigation once a week. Although standard practices will vary remarkably between farmers, this set-up forms a suitable baseline for establishing a framework to test the ability to use NWP to predict irrigation indices and measure the uncertainty of these predictions. Forecasts are issued daily over a 3.5-year period and therefore will cover a wide range of weather, soil, and crop states. A 40 mm irrigation is also applied at planting and ratooning to ensure that the water profile is initially full, and the crop does not fail to grow. Irrigation is stopped 60 days prior to harvesting to allow the crop to dry down before harvest. This dry down is often used in the region to increase sugar yields and coincides with the naturally dry time of year.

The APSIM model requires rainfall, maximum and minimum temperature and radiation data at a daily time step. “Observed” crop growth and soil parameters, for verification purposes, are taken as the simulations run using observed weather data. For each forecast date, forecasts and observations are simulated withholding the regular irrigation. This is so that forecast and observed conditions are not affected by the decision to irrigate and corresponds to the decision point, which is about timing and volume of irrigation in the next 7-day window.

For each forecast, APSIM simulations are warmed-up with observed data and up to the forecast issue date, after which models were run using the three sets of forecasts: no rainfall climatology (NRC, uninformative baseline), raw NWP and post-processed ensemble forecasts.

3.4. Irrigation decision indices

3.4.1. Total rainfall

Total rainfall over the next seven days is adopted as the single weather-based irrigation index. For each forecast model, total rainfall was calculated as the cumulative rainfall from the forecast date through to the next seven days as per equation 1.

$$\mathrm{TP}_j = \sum_{i=1}^{j} P_i \tag{1}$$

where TP is total precipitation and P_i is the daily precipitation.

3.4.2. Soil and crop indicators

Three APSIM model outputs are adopted as irrigation indices. These are soil water deficit (SWD), crop water use (CWU) and crop stress (Stress). Soil water deficit is taken as the difference between the field capacity and actual volume of water in the soil. SWD was calculated at the start of each day using two APSIM variables as per equation 2.

$$\mathrm{SWD} = D_{\mathrm{DUL}} - D \tag{2}$$

where D is the actual amount of water in the soil (mm) and D_{DUL} is the maximum possible amount of water at the drained upper limit (mm). These variables are reported by the APSIM soil water model as ‘sw_dep’ and ‘dul_dep’, respectively. CWU was estimated as the daily demand for soil water, which is directly reported by APSIM as ‘sw_demand’ (mm). Crop water demand in APSIM is calculated using the RUE/TE method (Wang et al., 2004). Crop Stress is estimated within APSIM as the effect of soil water stress on photosynthesis. This is reported directly by the APSIM sugar model as ‘swdef_photo’. We invert the default outputs so that the values range from 0 (unstressed) to 1 (fully stressed).

3.5. Skill assessment methods

Ensemble forecasts require verification with ensemble forecast verification measures. Here, we use the continuous ranked probability score (CRPS, Hersbach (2000)), a metric that combines information about the accuracy and reliability of ensemble forecasts. The average CRPS for T forecast events is defined in equation 3.

$$\mathrm{CRPS} = \frac{1}{T}\sum_{t=1}^{T}\int [F_t(y) - H(y - o_t)]^2 dy \tag{3}$$

with

$$H(y - o_t) = \begin{cases} 0 & \text{if } y < o_t \\ 1 & \text{if } y \geq o_t \end{cases}$$

where y is the prediction, o is the observation and F is the forecast cumulative distribution function (CDF). H is the CDF of the observation, characterised by the Heaviside step function.

The CRPS is a negatively oriented score such that a CRPS of zero indicates no error (i.e., perfectly accurate forecasts with no ensemble spread). In the case of deterministic forecasts, the CRPS reduces to the mean absolute error (MAE) as per equation 4.

$$\mathrm{MAE} = \frac{1}{T}\sum_{t=1}^{T}|y_t - o_t| \tag{3}$$

Reliability in the post-processed ensemble forecasts was assessed by analysis of the probability integral transform (PIT) (Laio & Tamea, 2007; Renard et al., 2010). The PIT of an observation given an ensemble forecast is defined as $\pi = F_t(y = o_t)$ where $F_t(y)$ is the cumulative distribution function of the ensemble forecasts and o_t is the corresponding observation for event t. For daily and total rainfall forecasts, when observed rainfall is zero, the cumulative probability represents a mass at zero. Therefore, $\pi = F_t(0)$ and it is necessary to sample a pseudo-PIT value uniformly within the range [0, π_t] (Wang & Robertson, 2011). Similarly, stress index values lie within a range [0, 1] and therefore a pseudo-PIT value is randomly selected from a range of [0,π_t] for observed values of 0. The upper limit is slightly more complicated; when the observation is at the upper limit, $\pi_t = F_t(y')$ where y' is the second

largest value in the forecast ensemble. A pseudo-PIT is uniformly sampled from the range $[\pi_t, 1]$.

Calculating PITs for soil water deficit presents a new problem that we believe has not been addressed in the literature. In simulations, there is effectively a lower bound on the soil moisture associated with zero rainfall and which places a dynamic upper bound on the soil water deficit and affects both F_t and o_t. This upper bound is detected computationally by checking for a probability mass at the maximum forecast soil water deficit value and, if the observation equals this bound, a pseudo-PIT is calculated in the range $[\pi_t, 1]$ in the same fashion as for the upper limit on crop stress.

If a forecasting system is reliable, π follows a standard uniform distribution. Reliability is visually examined by plotting the set of $\pi_t (t = 1, 2, \cdots, T)$ with the corresponding theoretical quantile of the uniform distribution in a QQ plot. Reliability is summarized using the α-index (Renard et al., 2010) as defined in equation 5.

$$\alpha = 1 - \frac{2}{T}\sum_{t=1}^{T}\left|\pi_t^* - \frac{t}{T+1}\right| \quad (5)$$

Where: π_t^* are the π_t sorted in increasing order. The α-index represents the deviation of π_t^* from the matching uniform distribution quantile in the QQ plot and ranges from 0 (completely unreliable) to 1 (completely reliable).

4. Results

4.1. Weather forecasts

Fig. 2 presents raw and post-processed weather forecasts for the Giru/Barratta region at a lead time of 3 days, along with scatter plots of the corresponding observations, plus the reliability of post-processed forecasts. The raw forecasts and observations are plotted with the Spearman correlation in the top row of Fig. 2. The forecasts for all four variables show moderate to high correlation, noting that a portion of the correlation is attributed to the seasonal cycle. We have not removed the effect of the seasonal cycle through anomaly correlation because the current forecast-processing does not model the seasonal cycle and the results are sufficient for the purpose of discerning the forecast performance for different weather variables. Possible improvements to account for the seasonal cycle will be discussed in section 4.

ACCESS-G3 has high raw correlation for Tmin and Tmax (correlations 0.94–0.95), with radiation showing moderate correlation (0.79) and rainfall weaker correlation (0.58). The second row of Fig. 2 shows that the forecast post-processing has converted the deterministic NWP forecast into an ensemble forecast with a representation of uncertainty. The reliability of the ensemble spread is formally assessed in the bottom row using PIT uniform probability plots and the PIT alpha metric. By both measures, the forecasts are exceptionally reliable in ensemble spread, with PIT alpha scores between 0.94–0.98. Despite overall reliability being high, the forecast and observations plots (middle row) suggest that the PITs may cluster depending on forecast magnitude; for

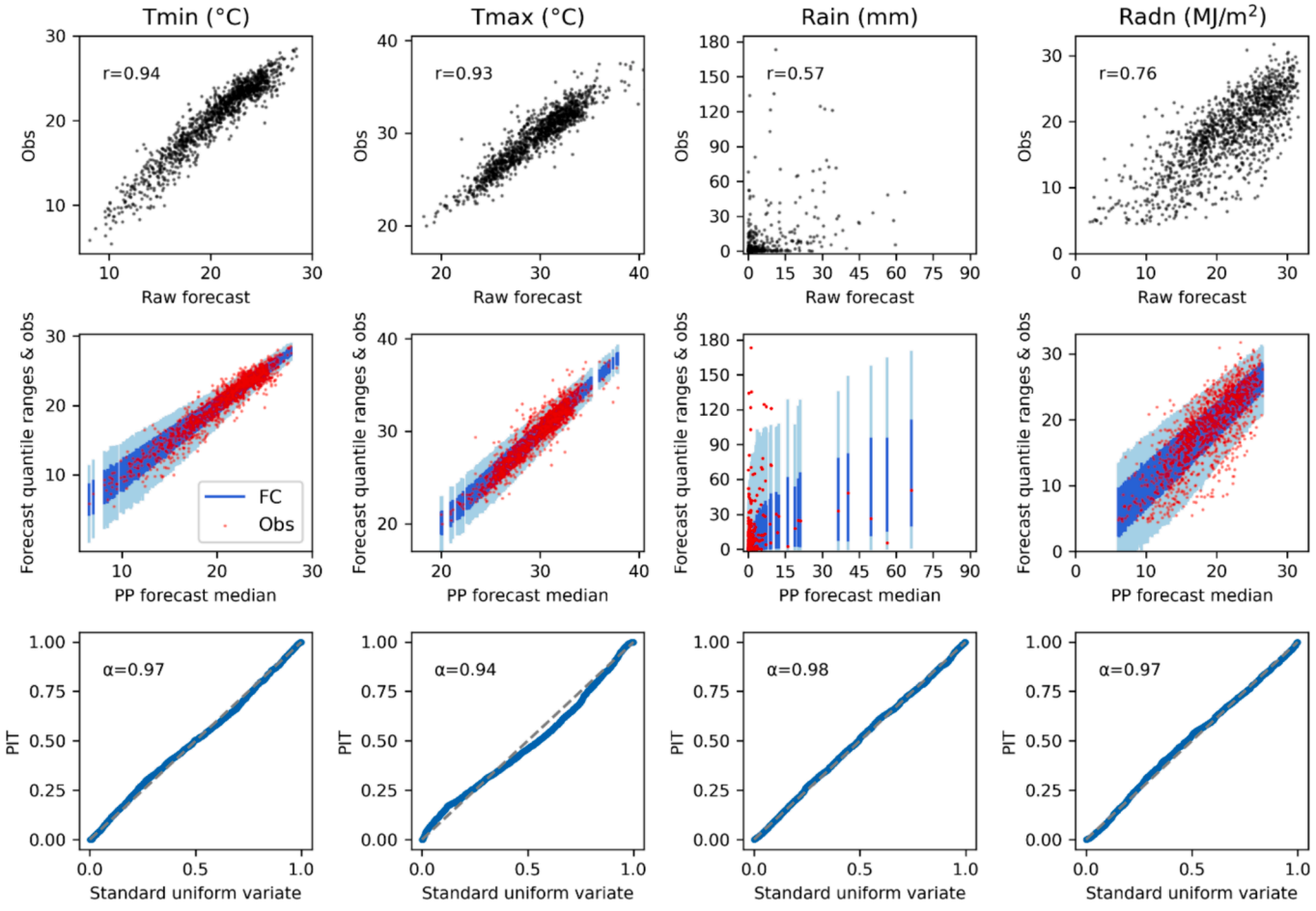

Fig. 2. . Weather forecasts, observations, and PIT reliability plots for the Giru/Barratta region at a lead time of 3 days. Top row: Scatterplot of raw ACCESS-G3 forecasts versus observations with the Spearman correlation. Middle row: post-processed forecast [0.25,0.75] and [0.05, 0.95] quantile ranges and observations plotted against forecast median. Bottom row: PIT uniform probability plots with the PIT alpha reliability metric.

example, for low Tmin. The problem and potential solutions are discussed further in section 4.

Raw and post-processed forecasts for all lead times from 1 to 7 days ahead and for all five climate zones are verified in Fig. 3. The raw ACCESS-G3 forecasts exhibit substantial bias for all forecast variables and varying degrees of bias between climate zones. Raw Tmin is systematically overpredicted by up to 10 % whereas raw Tmax is systematically underpredicted by up to 10 %. Raw rainfall is systematically underpredicted by up to 40 % and raw radiation is systematically overpredicted by about 20 %. The result for radiation is discussed further in section 4. After post-processing, Tmin, Tmax and radiation show little or no bias. Post-processed rainfall exhibits small biases, particularly for lead times from 3 to 7 days with biases up to 5–10 %. Bias in rainfall is harder to eliminate due to the non-normal nature of its distribution.

Forecast errors, being CRPS for the post-processed ensemble forecasts and MAE for the raw deterministic forecasts, show increasing magnitude with lead time and variance across climate zones. Post-processing improves forecast accuracy. Furthermore, post-processing reduces the spread in errors across climate zones for Tmin, Tmax and radiation. Forecasts for Tmin exhibit higher errors than forecasts for Tmax.

Consistent with the results in Fig. 2, reliability in ensemble spread is high for all weather variables and climate zones. A threshold for high reliability is selected as PIT-alpha = 0.9, which is based on familiarity with the relationship between PIT uniform probability plots and PIT-alpha scores. It can be seen in Fig. 2 that Tmax shows a small degree of under confidence (increased forecast uncertainty resulting in a forecast spread tending too wide) characterised by an "inverted S" shape to the PIT plot, which reduces the PIT-alpha to about 0.94. PIT values of about 0.9 or below indicate more serious problems with forecast spread or bias.

4.2. Irrigation-index forecasts

Fig. 4 presents forecasts, observations and reliability assessment of irrigation index forecasts at a lead time of 3 days in the Giru/Barratta region. Irrigation index forecasts are based on raw ACCESS-G3, a no rainfall climatology (NRC) weather forecast and the post-processed ACCESS-G3 forecasts. The observations in this case are pseudo-observations, that is, simulations using actual weather. The NRC-based forecasts (first row) show moderate to high correlation. Raw ACCESS-G3-based forecasts (second row) show moderate to high correlation amongst all irrigation indices, ranging from 0.73 for the three-day rainfall totals to 0.99 for soil water deficit. For crop water use and crop stress the raw correlations are higher than the NRC, signifying that the NWP forecasts add value when compared to an uninformative climatology-based approach. Correlation is not defined for the NRC three-day rainfall forecast since the NRC rainfall forecast is always zero. The post-processed-based forecasts (third row) show differences in

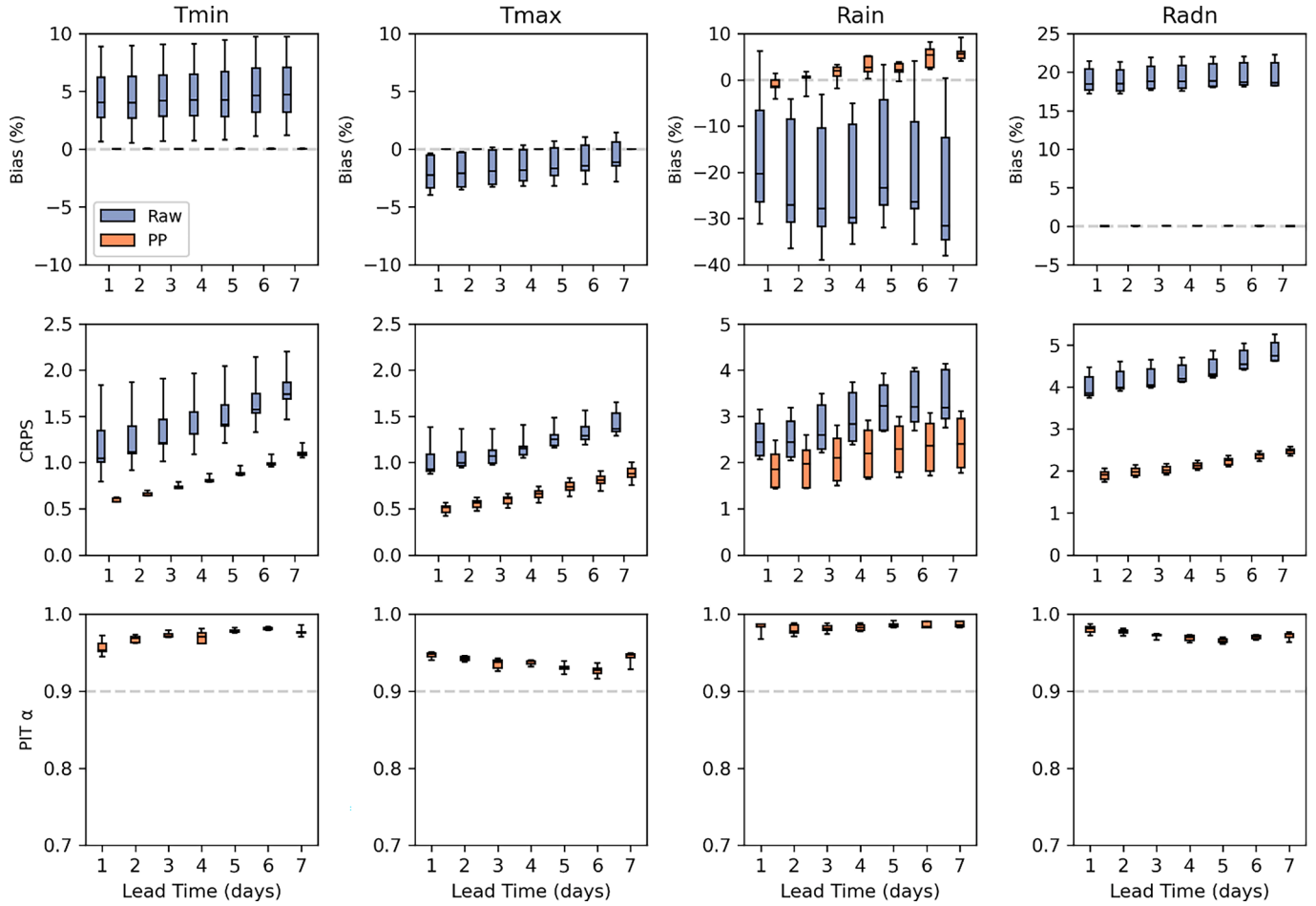

Fig. 3. . Bias, forecast error and reliability of weather forecasts for each forecast lead time from 1 to 7 days. Blue/first boxes represent raw ACCESS-G3 forecasts and black/second boxes represent post-processed forecasts. The spread of the boxplots represents the range of values for the five climate zones. Whiskers are the minimum and maximum values, boxes are the second smallest/largest values and the line is the median value. Top row: Bias as a percentage with ideal bias (0) marked as a dashed line. Middle row: CRPS for ensemble forecasts and MAE for deterministic forecasts. Bottom row: PIT alpha summarising reliability with a dashed line at 0.9 identifying the high reliability zone (reliability applies to ensemble forecasts only).

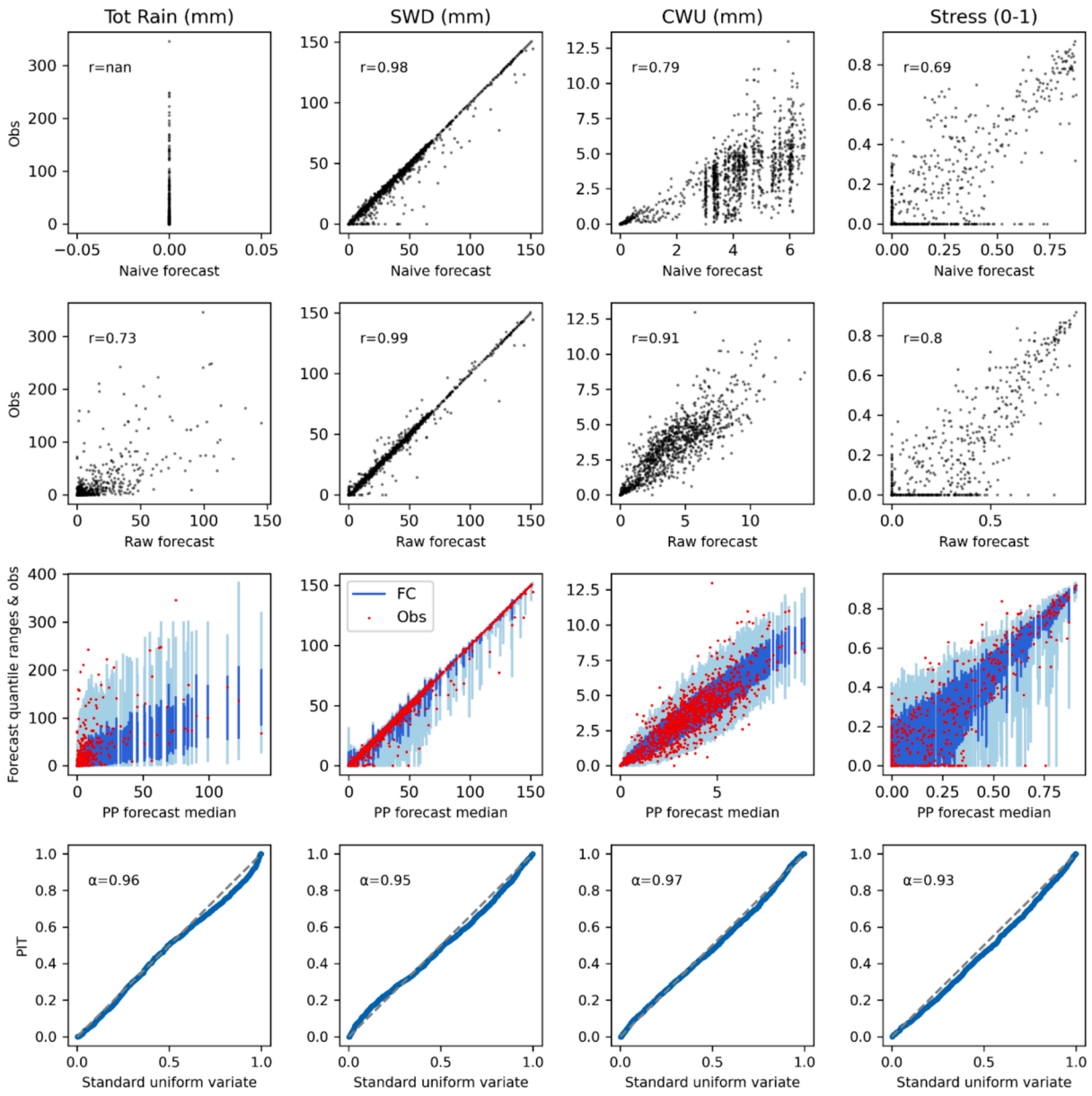

Fig. 4. . Irrigation index forecasts, observations, and PIT reliability plots for the Giru/Barratta region at a lead time of 3 days. Top row: Scatterplot of raw NRC forecasts versus observations with the Spearman correlation. Second row: Scatterplot of raw ACCESS-G3-based forecasts versus observations with the Spearman correlation. Third row: Post-processed-based forecast [0.25,0.75] and [0.05, 0.95] quantile ranges and observations plotted against forecast median. Bottom row: PIT uniform probability plots with the PIT alpha reliability metric.

uncertainty depending on the forecast variable and the magnitude of the forecast. For soil water deficit, the uncertainty is frequently very narrow around the current value, with expansions to lower SWD (presumably) associated with an increased probability of rainfall. Forecasts of CWU and Stress show consistently higher uncertainty, reflecting their more dynamic nature. In all cases, the forecasts of irrigation indices show high reliability in ensemble spread at three days lead time, with PIT-alpha in the range 0.95–0.96.

Fig. 5 summarises the performance of the irrigation index forecasts for all five climate zones and forecast lead times. Bias (first row) and forecast accuracy (CRPS/MAE, second row) both show considerable variability between climate zones (wide boxes in boxplots). Raw rainfall totals consistently underpredict (except in a few cases) up to 40 % and NRC rainfall totals underpredict by 100 % (by definition). The under-predictions in raw and naïve rainfall totals are associated with over-predictions of soil water deficit, particularly in the NRC case, which grows into a bias of up to 20 % at day 7. Post-processed rainfall forecasts show limited bias with a trend towards positive bias in accumulated rainfall somewhat associated with a negative trend towards lower soil water deficit. Post-processed forecasts show little bias for crop water use and crop stress, whereas raw and NRC forecasts exhibit biases of up to 20 % for crop water use and up to 40 % for crop stress. In all cases, post-processed forecasts demonstrate the best forecast accuracy for all lead times and irrigation indices (second row), with the raw forecasts consistently outperforming NRC forecasts. Reliability is above the threshold of PIT-alpha = 0.9 for all variables and lead times except for total rainfall at days 6 and 7. The reliability of accumulated rainfalls depends on the Schaake Shuffle and is discussed further in section 4.

5. Discussion

5.1. Improvement of post-processed weather forecasts

Post-processed forecasts were always an improvement over both no

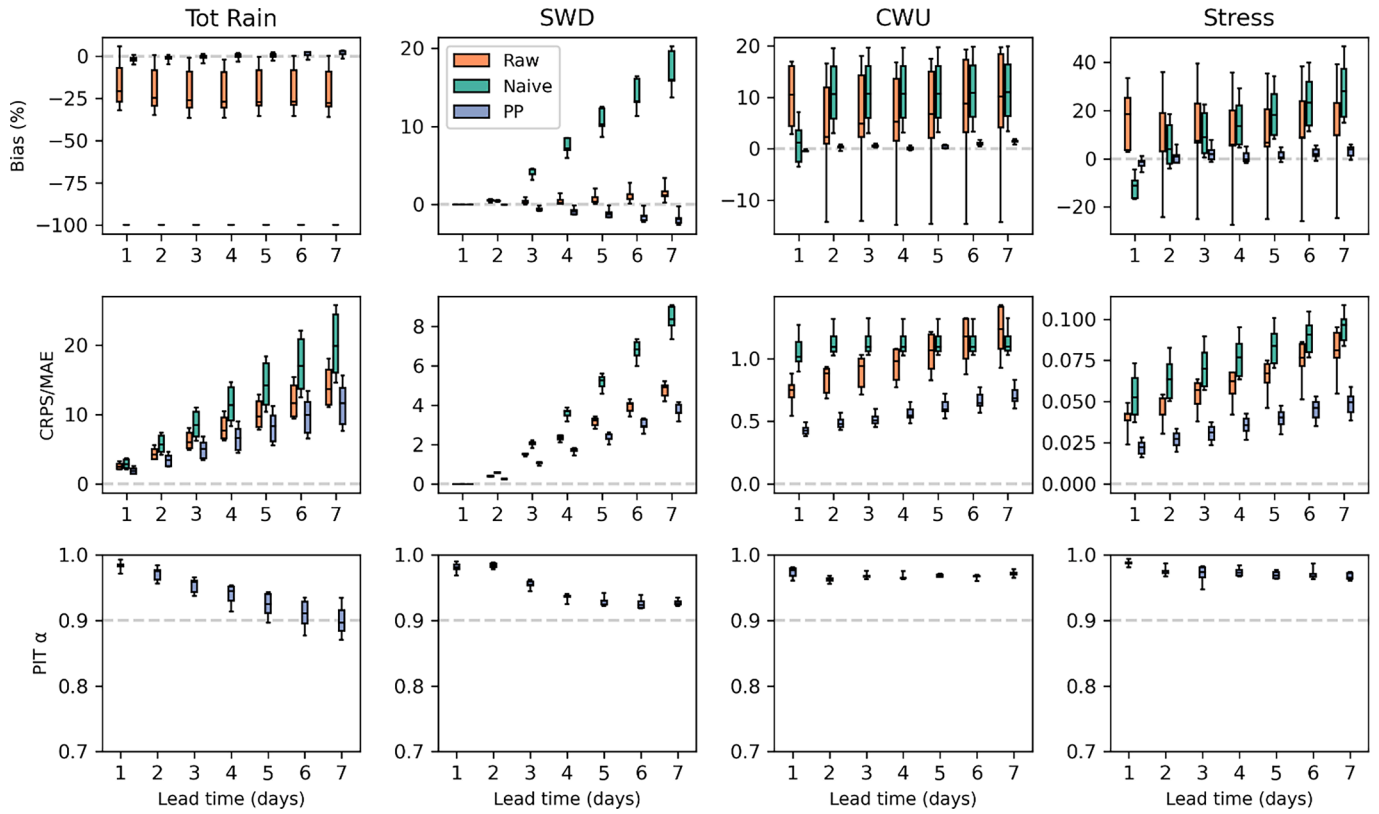

Fig. 5. . Bias, forecast error and reliability of irrigation index forecasts for each forecast lead time from 1 to 7 days. Blue/first boxes represent raw ACCESS-G3-based forecasts, red/second boxes represent naïve-based forecasts and black/third boxes represent post-processed forecasts. The spread of the boxplots represents the range of values for the five climate zones. Whiskers reach the minimum and maximum values. Top row: Bias as a percentage with ideal bias (0) marked as a dashed line. Middle row: CRPS for ensemble forecasts and MAE for deterministic forecasts. Bottom row: PIT alpha summarising reliability with a dashed line at 0.9 identifying the high reliability zone (reliability applies to ensemble forecasts only).

rainfall climatology (NRC) and raw ACCESS-G forecasts. As was expected, post-processing of the raw forecasts reduced forecast bias, in some cases considerably. The reduction in bias and error (CRPS) at longer lead times can be especially advantageous for planning of irrigation and other crop management decisions. The decision support tool Opticane (Sexton et al., 2022), co-designed with industry partners, shows how many farm management tasks such as spraying, harvesting, fertilizing as well as irrigation are dependent on weather conditions. Improved accuracy and reliability at longer lead times means a better ability to plan management decisions. This can be particularly useful for large farming systems that must manage a substantial number of paddocks, that may be spread across different climate zones. While many management decisions are dependent solely on weather, irrigation decisions can be more nuanced, depending on the state of the soil.

5.2. *Limitations in weather forecasts*

An important consideration in assessing post-processing skill is the 'ground-truth' data used. In this study SILO data were used as the 'true' representation of weather in each region. This data set is convenient, freely available and of high spatial resolution. However, gridded SILO products may systematically over- or under-estimate observations relative to weather station records in the region. For example, SILO radiation used in this study is calculated predominantly from cloud cover with some radiometry. A prominent negative bias has developed in recent years in comparison with historical data and satellite estimates. This is due to a reduction in ground-based radiometers that SILO relied on. Since the conclusion of this study, SILO has been updated with satellite measurements after 1990. The impact on our study is that the overestimation of radiation by the raw ACCESS-G forecasts is inflated to some degree. Nevertheless, in post-processing to match SILO data, the forecasts were 'improved' as they better match the existing SILO records. Furthermore, the method presented can be applied to downscale forecasts to a local, on-farm, weather station, thus providing the most relevant forecasts for a farming enterprise.

Despite high overall reliability of the post-processed forecasts, there is evidence of clustering in some PIT values for the post-processed Tmin and, to a lesser degree, Tmax and radiation values, which suggests that the use of a single transformation and post-processing model for all months of the year is not ideal. Possible fixes include applying the post-processing model to each month or season of the year independently, although this reduces that amount of data available for model training. Alternatively, incorporating a seasonal cycle into the post-processing model would allow use of all the training data whilst modelling the seasonal cycle. This would have the added advantage of making the forecasts approach a seasonal climatology rather than an annual climatology as skill reduces (e.g. Wang, Zhao, et al., 2019), which may improve skill and reliability further. We are currently investigating such a revised weather post-processing model.

As noted in the methods, each post-processed weather forecast ensemble at each lead time is produced independently, meaning the ensemble members are not initially sequential across lead times. The Schaake Shuffle attempts to correct for this by imposing historical trends on the ensemble values, allowing us to calculate realistic cumulative values such as total rainfall. While post-processed reliability for total rainfall was lower than other weather and irrigation indices, without the use of the Schaake Shuffle, reliability would be much harder to achieve. Fig. 6 demonstrates this, with reliability unacceptable beyond 2 days lead time when the Schaake Shuffle is not applied.

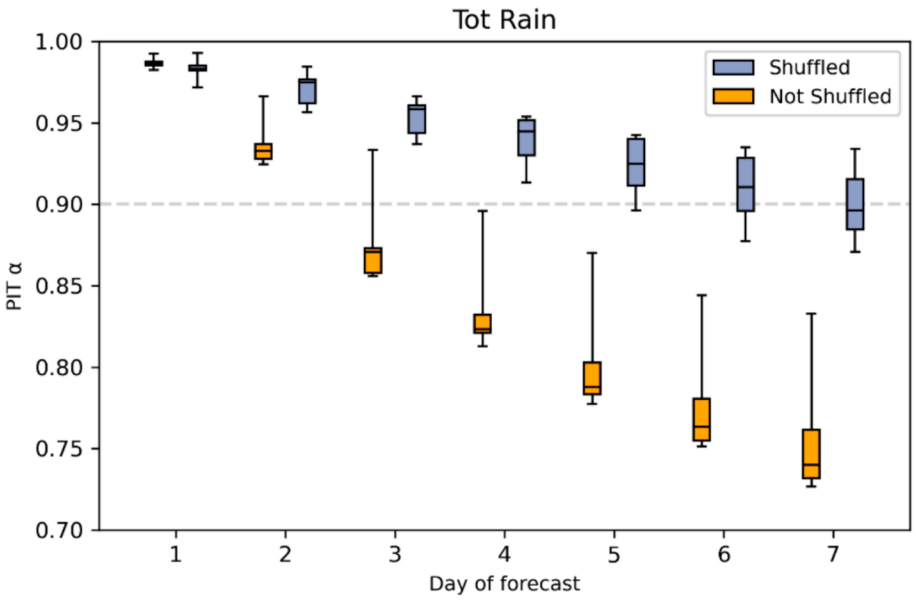

Fig. 6. PIT alpha reliability metric for cumulative rainfall with and without applying the Schaake Shuffle to connect ensemble members across lead times. Boxplots depict the range for the five climate zones. A dashed line at 0.9 indicates high reliability.

5.3. Impacts for irrigation decisions

The results presented justify the use of post-processed forecasts in developing irrigation schedules. While previous research has shown that including forecasts could be used to optimize irrigation schedules (Cao et al., 2019; Guo et al., 2022), it is important to understand how skill and uncertainty in the weather forecasts affects irrigation decision indices. In our study, results for raw ACCESS-G forecasts suggest routine enhancement of value in post-processing CWU and Stress, allowing the decision maker to regularly adjust irrigation volumes, for example. On the other hand, SWD is highly predictable under a no rain scenario (which is usually the case), and therefore the value is associated with rarer large rainfall events, which allow the decision maker to entertain decisions such as delaying irrigation. Post-processed forecasts may also assist with decision making for pesticide and fertiliser application and burning and harvesting the cane.

While improved forecast lead times obtained by post-processing forecasts is important for scheduling, the potential impact in terms of yield and water savings still needs to be investigated. Quantifying the impact of improved forecasts will need to consider the practical limitations farm managers must contend with. Irrigation scheduling at longer lead times may only be practically advantageous when the infrastructure exists to effectively manage the amount and timing of irrigation events. For example, automated irrigation systems such as described by Wang et al. (2020) could incorporate forecast weather or decision indices to optimize irrigation schedules where irrigation events can be fully automated. When investigating the potential impact of including forecasts in irrigation scheduling, researchers should consider both automated and manual irrigation scenarios to develop decision rules that are appropriate for different systems in the study region. Furthermore, there may be system scale benefits where predictable irrigation demand allows water authorities to manage water supply more efficiently.

6. Conclusion

Improved, locally relevant short-range weather forecasts are essential to improving agricultural management decisions. While there is a growing body of research on the impact of incorporating weather forecasts into management decision support tools for decisions such as irrigation scheduling, there is often a lack of investigation on how skill in weather forecasts translates to skill in decision indices. This manuscript outlines a methodology for developing locally relevant post-processed forecasts and assesses the skill of these forecasts for weather variables and derived indices. Post-processed forecasts showed improved weather forecast skill (CRPS) relative to raw forecasts and high reliability. Raw forecasts of SWD and Stress indices have large biases and poor accuracy, especially at longer lead times. However, we show that by post-processing weather forecasts it is possible to provide improved weather forecasts and longer lead times. We also show that deterministic forecasts can be converted to ensemble forecasts that can be used to produce reliable forecasts of irrigation indices using a crop model. Future research can investigate the impact of optimizing irrigation schedules using these forecasts. However, such future research must consider practical constraints on irrigation systems used in the target region.

CRediT authorship contribution statement

Andrew Schepen: Visualization, Validation, Software, Methodology, Investigation, Formal analysis, Data curation, Conceptualization, Writing – original draft, Writing – review & editing. **Justin Sexton:** Conceptualization, Data curation, Formal analysis, Investigation, Methodology, Software, Validation, Visualization, Writing – original draft, Writing – review & editing. **Bronson Philippa:** Writing – review & editing, Supervision, Project administration, Methodology, Conceptualization, Formal analysis. **Steve Attard:** Writing – review & editing, Resources, Investigation, Conceptualization. **David E. Robertson:** Writing – review & editing, Visualization, Validation, Methodology. **Yvette Everingham:** Writing – review & editing, Writing – original draft, Visualization, Validation, Supervision, Methodology, Investigation, Funding acquisition, Conceptualization.

Declaration of competing interest

The authors declare that they have no known competing financial interests or personal relationships that could have appeared to influence the work reported in this paper.

Data availability

Data will be made available on request.

Acknowledgements

ACCESS-G data was sourced from the Bureau of Meteorology and the National Computational Infrastructure. Silo data was sourced from the Queensland Government. This research was conducted under the Climate Smart Sugarcane Irrigation Partnerships project funded by the Australian Government National Landcare Program (grant agreement 4-99YFDKA). We thank two anonymous reviewers for their valuable comments to improve upon the original manuscript.

References

Anupoju, V., Kambhammettu, B.P., Regonda, S.K., 2021. Role of short-term weather forecast horizon in irrigation scheduling and crop water productivity of rice. J. Water Resour. Plan. Manag. 147 (8), 05021009.

Belaud, G., Mateos, L., Aliod, R., Buisson, M.C., Faci, E., Gendre, S., Ghinassi, G., Gonzales Perea, R., Lejars, C., Maruejols, F., 2020. Irrigation and energy: issues and challenges. Irrig. Drain. 69, 177–185.

Cao, J., Tan, J., Cui, Y., Luo, Y., 2019. Irrigation scheduling of paddy rice using short-term weather forecast data. Agric Water Manag 213, 714–723. https://doi.org/10.1016/j.agwat.2018.10.046.

Clark, M., Gangopadhyay, S., Hay, L., Rajagopalan, B., Wilby, R., 2004. The Schaake shuffle: A method for reconstructing space-time variability in forecasted precipitation and temperature fields. J. Hydrometeorol. 5 (1), 243–262.

Department of Environment and Science, 2023. *Land use Mapping Series*. State of Queensland. http://qldspatial.information.qld.gov.au/catalogue/custom/search.page?q=%22Land use mapping series%22.

Domínguez-Niño, J.M., Oliver-Manera, J., Girona, J., Casadesús, J., 2020. Differential irrigation scheduling by an automated algorithm of water balance tuned by capacitance-type soil moisture sensors. Agric. Water Manag. 228, 105880.

Fader, M., Shi, S., von Bloh, W., Bondeau, A., Cramer, W., 2016. Mediterranean irrigation under climate change: more efficient irrigation needed to compensate for increases in irrigation water requirements. Hydrol. Earth Syst. Sci. 20 (2), 953–973. https://doi.org/10.5194/hess-20-953-2016.

Gedam, S., Pallam, H., Kambhammettu, B.V.N.P., Anupoju, V., Regonda Satish, K., 2023. Investigating the accuracies in short-term weather forecasts and its impact on irrigation practices. J. Water Resour. Plan. Manag. 149 (2), 04022079. https://doi.org/10.1061/JWRMD5.WRENG-5644.

Goap, A., Sharma, D., Shukla, A.K., Krishna, C.R., 2018. An IoT based smart irrigation management system using Machine learning and open source technologies. Comput. Electron. Agric. 155, 41–49.

Gu, Z., Qi, Z., Burghate, R., Yuan, S., Jiao, X., Xu, J., 2020. Irrigation scheduling approaches and applications: a review. J. Irrigation Drainage Eng. 146 (6), 04020007. https://doi.org/10.1061/(asce)ir.1943-4774.0001464.

Gu, Z., Zhu, T., Jiao, X., Xu, J., Qi, Z., 2021. Neural network soil moisture model for irrigation scheduling. Comput. Electron. Agric. 180, 105801.

Guo, D., Wang, Q.J., Ryu, D., Yang, Q., Moller, P., Western, A.W., 2022. An analysis framework to evaluate irrigation decisions using short-term ensemble weather forecasts. Irrig. Sci. https://doi.org/10.1007/s00271-022-00807-w.

Hersbach, H., 2000. Decomposition of the continuous ranked probability score for ensemble prediction systems. Weather Forecast. 15 (5), 559–570.

Holzworth, D., Huth, N.I., Fainges, J., Brown, H., Zurcher, E., Cichota, R., Verrall, S., Herrmann, N.I., Zheng, B., Snow, V., 2018. APSIM next generation: overcoming challenges in modernising a farming systems model. Environ. Model. Softw. 103, 43–51. https://doi.org/10.1016/j.envsoft.2018.02.002.

Jiang, Z., Johnson, F., 2023. A new method for postprocessing numerical weather predictions using quantile mapping in the frequency domain. Mon. Weather Rev. 151 (8), 1909–1925. https://doi.org/10.1175/MWR-D-22-0217.1.

Keating, B.A., Robertson, M.J., Muchow, R.C., Huth, N.I., 1999. Modelling sugarcane production systems I. Development and performance of the sugarcane module. Field Crop Res 61 (3), 253–271. https://doi.org/10.1016/S0378-4290(98)00167-1.

Laio, F., Tamea, S., 2007. Verification tools for probabilistic forecasts of continuous hydrological variables. Hydrol. Earth Syst. Sci. 11 (4), 1267–1277.

Lakatos, M., Lerch, S., Hemri, S., Baran, S., 2023. Comparison of multivariate post-processing methods using global ECMWF ensemble forecasts. Q. J. R. Meteorolog. Soc. 149 (752), 856–877.

Lisson, S.N., Robertson, M.J., Keating, B.A., Muchow, R.C., 2000. Modelling sugarcane production systems: II: Analysis of system performance and methodology issues. Field Crop Res 68 (1), 31–48. https://doi.org/10.1016/S0378-4290(00)00108-8.

Potgieter, A.B., Schepen, A., Brider, J., Hammer, G.L., 2022. Lead time and skill of Australian wheat yield forecasts based on ENSO-analogue or GCM-derived seasonal climate forecasts–A comparative analysis. Agric. For. Meteorol. 324, 109116.

Renard, B., Kavetski, D., Kuczera, G., Thyer, M., Franks, S.W., 2010. Understanding predictive uncertainty in hydrologic modeling: The challenge of identifying input and structural errors. Water Resour. Res. 46 (5).

Robertson, D.E., Shrestha, D.L., Wang, Q.J., 2013. Post-processing rainfall forecasts from numerical weather prediction models for short-term streamflow forecasting. Hydrol. Earth Syst. Sci. 17 (9), 3587–3603. https://doi.org/10.5194/hess-17-3587-2013.

Rosa, L., Gabrielli, P., 2023. Achieving net-zero emissions in agriculture: a review. Environ. Res. Lett. 18 (6), 063002 https://doi.org/10.1088/1748-9326/acd5e8.

Schepen, A., Everingham, Y., Wang, Q.J., 2020a. Coupling forecast calibration and data-driven downscaling for generating reliable, high-resolution, multivariate seasonal climate forecast ensembles at multiple sites [Article]. Int. J. Climatol. 40 (4), 2479–2496. https://doi.org/10.1002/joc.6346.

Schepen, A., Everingham, Y., Wang, Q.J., 2020b. An improved workflow for calibration and downscaling of GCM climate forecasts for agricultural applications – A case study on prediction of sugarcane yield in Australia. Agric. For. Meteorol. 291, 107991 https://doi.org/10.1016/j.agrformet.2020.107991.

Schepen, A., Everingham, Y., Wang, Q.J., 2020c. On the joint calibration of multivariate seasonal climate forecasts from GCMs. Mon. Weather Rev. 148 (1), 437–456.

Sexton, J., Everingham, Y., Skocaj, D., Biggs, J. S., Thorburn, P., Schroeder, B., 2017. Identification of climatological sub-regions within the tully mill area. Proceedings of the Australian Society of Sugar Cane Technologists, Cairns, Queensland, Australia.

Sexton, J., Melville, B., Schepen, A., Philippa, B., Attard, S., Davis, M., Everingham, Y., 2022. *Opticane: an irrigation and weather support tool* Australian Society of Sugar Cane Technologists.

Shrestha, D.L., Robertson, D.E., Bennett, J.C., Wang, Q., 2015. Improving precipitation forecasts by generating ensembles through postprocessing. Mon. Weather Rev. 143 (9), 3642–3663.

Sun Water, 2022. *Burdekin Falls Dam Fact Sheet: Raising Project*. Sun Water. Retrieved 2023-11-23 from https://www.sunwater.com.au/wp-content/uploads/Home/Projects/Burdekin-Falls-Projects/Burdekin_Falls_Dam_Raising_Fact_Sheet_December_2022.pdf.

Wang, E., Smith, C.J., Bond, W.J., Verburg, K., 2004. Estimations of vapour pressure deficit and crop water demand in APSIM and their implications for prediction of crop yield, water use, and deep drainage. Aust. J. Agr. Res. 55 (12), 1227–1240. https://doi.org/10.1071/AR03216.

Wang, E., Attard, S., Linton, A., McGlinchey, M., Xiang, W., Philippa, B., Everingham, Y., 2020. Development of a closed-loop irrigation system for sugarcane farms using the Internet of Things. Comput. Electron. Agric. 172, 105376 https://doi.org/10.1016/j.compag.2020.105376.

Wang, D., Cai, X., 2009. Irrigation scheduling—role of weather forecasting and farmers' behavior. J. Water Resour. Plan. Manag. 135 (5), 364–372.

Wang, Q.J., Robertson, D.E., 2011. Multisite probabilistic forecasting of seasonal flows for streams with zero value occurrences. Water Resour. Res. 47 (2) https://doi.org/10.1029/2010WR009333.

Wang, Q., Shrestha, D.L., Robertson, D., Pokhrel, P., 2012. A log-sinh transformation for data normalization and variance stabilization. Water Resour. Res. 48 (5).

Wang, Q., Shao, Y., Song, Y., Schepen, A., Robertson, D.E., Ryu, D., Pappenberger, F., 2019a. An evaluation of ECMWF SEAS5 seasonal climate forecasts for Australia using a new forecast calibration algorithm. Environ. Model. Softw. 122, 104550.

Wang, Q., Zhao, T., Yang, Q., Robertson, D., 2019b. A seasonally coherent calibration (SCC) model for postprocessing numerical weather predictions. Mon. Weather Rev. 147 (10), 3633–3647.

Waterhouse, J., Schaffelke, B., Bartley, R., Eberhard, R., Brodie, J., Star, M., Thorburn, P., Rolfe, J., Ronan, M., Taylor, B., Kroon, F., 2017. *2017 Scientific Consensus Statement: Land use impacts on Great Barrier Reef water quality and ecosystem condition*. T. S. O. Queensland. https://www.reefplan.qld.gov.au/_data/assets/pdf_file/0029/45992/2017-scientific-consensus-statement-summary.pdf.

Whan, K., Zscheischler, J., Jordan, A.I., Ziegel, J.F., 2021. Novel multivariate quantile mapping methods for ensemble post-processing of medium-range forecasts. Weather Clim. Extremes 32, 100310.

Yeo, I.K., Johnson, R.A., 2000. A new family of power transformations to improve normality or symmetry. Biometrika 87 (4), 954–959.

Zhao, P., Wang, Q.J., Wu, W., Yang, Q., 2022. Spatial mode-based calibration (SMoC) of forecast precipitation fields from numerical weather prediction models. J. Hydrol. 613, 128432 https://doi.org/10.1016/j.jhydrol.2022.128432.